AN ON-LINE DETECTION METHOD FOR CONVEYOR BELT DEVIATION FAULTS

by

Mingsheng LIU[c], Xiuzhuang MEI[a,b*], DongMing SUN[c], Jian ZHANG[c], and Zelin CHEN[b]

[a] School of Mechanical Engineering, Inner Mongolia University of Technology, Hohhot, China
[b] Inner Mongolia Dazhi Energy Technology Co., Ltd., Hohhot, China
[c] Inner Mongolia Daban Power Generation Co., Ltd., Chifeng, China

Original scientific paper
https://doi.org/10.2298/TSCI2303099L

The conveyor belt deviation occurs frequently, and it will finally lead to an accident, so its detection has triggered skyrocketing attention from both industry and academia. In this paper, an adaptive segmentation model and a belt offset quantification model are established for continuous online detection of the conveyor belt deviation status. The results show that the degree of the conveyor belt deviation can be quantitatively calculated and its deviation status can be objectively evaluated. This technology has opened the path for a new way to on-line continuously detect the conveyor belt deviation.

Key words: *conveyor belt, deviation, adaptive segmentation, machine vision*

Introduction

Belt conveyors, as an important equipment for bulk material transportation, are widely applied in the fields of coal, metallurgy, mining, electric power, and building materials owing to their advantages in long transportation distance, large transportation volume, stable operation, and convenient loading and unloading. The conveyor belt is a critical carrying and traction component, whose safe and stable operation affects directly the production safety and economic benefits. Since belt conveyors work in a complex and harsh environment and run at high loads for prolonged time, conveyor belt faults are frequently encountered, among which the deviation fault is the most common one [1, 2]. If the deviation fault is not discovered and handled timely, it will cause material spilling and aggravate rubber abrasion in less severe cases, which leads to material loss and low production efficiency, and the belt service life will be also greatly affected. In more severe cases, the conveyor belt will roll and hang up to cause longitudinal tearing, which leads to human casualty and equipment damage, and huge economic losses occur, thereby production safety is seriously affected. Hence, real-time monitoring of the conveyor belt deviation fault is necessary during operation. Once the deviation occurs, an alarm or shutdown should be activated timely to avoid major accidents.

Currently, the deviation detection devices for conveyor belts in engineering practices adopt mostly deviation switches. Upon occurrence of instantaneous deviation or presence of a large material block on the conveyor belt edge, the belt or material block often collides with the deviation switch, causing false alarms. Its false alarm rate is too high to prevent the dam-

* Corresponding author, e-mail: mxz@imut.edu.cn

age easily, and people suffering from the false alarms lack an immediate action when the danger is approaching. As a qualitative detection device, the deviation switch often detects only two fixed deviation positions, and it is incapable of monitoring the continuous position change of conveyor belt operation center, and thus cannot accurately assess the degree of deviation. Given the inefficient detection of deviation faults, the longitudinal tearing accident of conveyor belts occurs occasionally. Hence, this paper aims to improve the accuracy of deviation fault identification by achieving the real-time monitoring of conveyor belt center position and the quantitative description of deviation degree, which is conducive to enhancing the conveying efficiency of conveyor belts and ensuring their safe and stable operation.

The conveyor belt deviation detection technology has received skyrocketing attention from industrial and academic communities. Several authors [3-5] have carried out research on the mechanism of the conveyor belt deviation and suggested an automatic correction method to find relationship among various parameters, *e.g.* the belt material parameters, dynamic parameters, and speed. Gao *et al.* [6] used a multi-view adaptive image enhancement algorithm to suppress the impact of uneven illumination, which laid a foundation for detecting conveyor belt faults like deviation and surface damage. Zhang *et al.* [7] developed a deviation detection system using a line laser generator and LABVIEW platform, which achieved reliable real-time detection of conveyor belt deviation faults. Zeng *et al.* [8] proposed a real-time conveyor belt detection algorithm based on multi-scale feature fusion network, and optimized the network with a novel weighted loss function, thereby the detection efficiency of conveyor belt edges was remarkably improved. Yang *et al.* [9] proposed a fast image segmentation algorithm to monitor the longitudinal tear and deviation of the conveyor belt. Yang *et al.* [10] adopted the improved Hough Transform algorithm to extract the belt deviation characteristics. A detection method of coal quantity and deviation of belt conveyor based on multi-task convolutional neural network was proposed in [11]. Currently, all of the mentioned methods are in the laboratory research phase, so their adaptability and reliability to practical engineering applications deserve further exploration.

Image acquisition device

In order to obtain the dynamic offset information about the conveyor belt, this study uses an image acquisition device which is installed between the upper and lower belts. Three linear LED light sources and a linear array charge coupled device (CCD) camera with 2048 px and a maximum line frequency of 19 kHz are used. The structural arrangement is shown in fig. 1. The linear light Source 2 is placed transversely, and the linear light Sources 1 and 3 are placed obliquely. The position is generally similar to the arc shape of the conveyor belt.

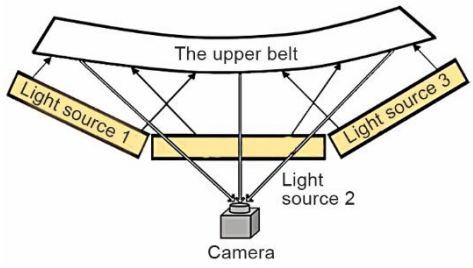

Figure 1. Image acquisition devices for monitoring conveyor belt deviation

Adaptive segmentation algorithm for conveyor belt images

The imaging technology is widely used in health analysis [12-18]. The line scan camera captures continuously images along the width direction of the conveyor belt, a row of pixels is constituted for the belt image. By continuous capturing of the conveyor belt in opera-

tion, a frame of image $I(i, j)$ is formed, where $i < H$, $j < W$, and H, W denote the height and width of the image, respectively. The reflected light intensity of the j^{th} point of linear light source after irradiating the rubber surface is defined as $y(j)$. With the operation of the conveyor belt, the light intensity is received by the j^{th} phase element of the linear array camera, which outputs the j^{th} column of the conveyor belt image. Clearly, the mean gray value $m(j)$ of pixels in the image j^{th} column is directly proportional to the value of $y(j)$, that is, $m(j) \propto y(j)$. Normally, the detection target's response $y(j)$ to light intensity is rather strong, while the response of non-detection objects is rather weak. A response greater than $k_1 y(j)$ can be regarded as the detection target-related part. Otherwise, it is a non-detection object. Here $k_1 \in [0,1]$ and $k_1 y(j) \propto k_1 m(j)$, so $k_1 m(j)$ can be used as a discrimination threshold between the image foreground and background.

The mean column vector of conveyor belt image $I(i, j)$ is computed:

$$m(j) = \frac{1}{H}\sum_{i=1}^{H} I(i, j), \quad j = 1, 2, 3, \cdots, W \tag{1}$$

The foreground and background attributes of image can be expressed:

$$z(i, j) = \text{sign}[I(i, j) - k_1 m(j)] \tag{2}$$

If $z(i, j) = 1$, it represents the image foreground; otherwise, $z(i, j) = 0$ or -1 represents the image background.

A segmentation model for conveyor belt images is built, and the model output $I_o(i, j)$ is:

$$I_o(i, j) = 0.5 - 0.5\text{sign}[I(i, j) - 0.5z(i, j)m(j) + \varepsilon] \tag{3}$$

where ε denotes an arbitrary minimum value greater than zero.

To solve the adjustment coefficient k_1, an objective function is created:

$$O(I_o) = 10/\text{En}(I_o) + \text{Area}(I_o) + 0.7\text{Std}(I_o) \tag{4}$$

where $\text{En}(I_o) = -\Sigma_{n=0}^{255} p_n \log_2 p_n$, p_n denotes the appearance probability of gray value n. The area and standard deviation of image I_o obtained by $\text{Area}(I_o)$ and $\text{Std}(I_o)$, respectively. That is capable of minimizing the objective function $O(I_o)$ upon obtaining the optimal parameter $\{k_1^*\}$.

Finally, by taking eq. (4) as the objective function, the adjustment coefficient of the segmentation model in eq. (3) is solved with the artificial bee colony algorithm, where the total number of bee colonies is set to 40, the total number of nectar sources is 20, the maximum iteration times are 10, and the maximum update times 10.

Taking the conveyor belt image with uneven illumination in fig. 2(a) as an example, fast image segmentation during deviation fault detection is illustrated. As shown in fig. 2(b), the attributes $z(i, j)$ of foreground and background in fig. 2(a) are computed, where the part with high brightness represents foreground, and the rest represents background. Using the artificial bee colony algorithm, the parameter value of k_1 is calculated to be 0.52, and fig. 2(c) presents the image segmentation result. Clearly, the left and right edges of the conveyor belt are very distinct. Through column projection, the position co-ordinates of belt left and right edges can be easily obtained. Figure 2(d) is derived by performing column projection and normalization on fig. 2(c). Based on the figure, the left and right edge co-ordinates of the conveyor belt are computed as Lx = 91 px and Rx = 402 px, respectively.

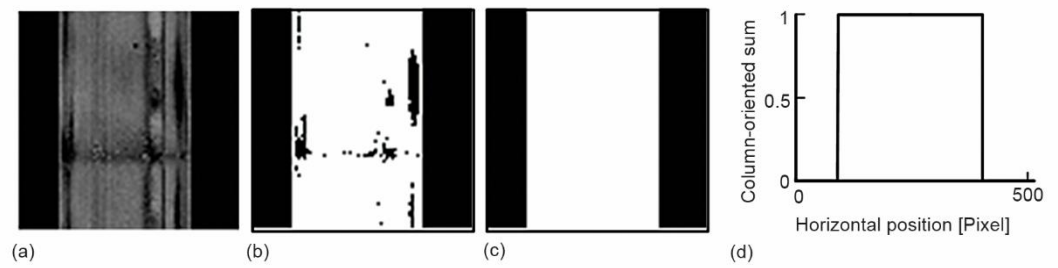

Figure 2. Fast detection of conveyor belt edge; (a) original image, (b) foreground and background attributes, (c) segmentation result, and (d) vertical projection of image (c)

Computation of global conveyor belt offset

The deviation fault of conveyor belt is characterized by a serious global deviation in the belt, which is represented by the deviation schematic shown in fig. 3. The central co-ordinate of the conveyor belt runway is O, and the central co-ordinate of the conveyor belt following global offset is O_1. Besides, the left and right edge co-ordinates of the rectangle circumscribed by the conveyor belt are Lx and Rx, respectively.

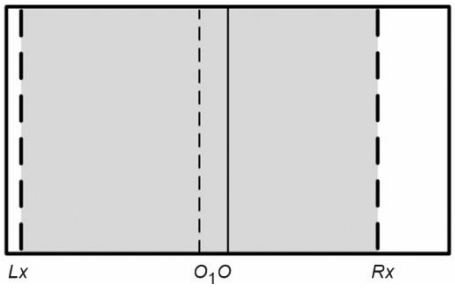

Figure 3. Schematic of conveyor belt deviation

Prior to detecting the belt deviation fault, it is necessary to determine the central co-ordinates of runway and the reference bandwidth of conveyor belt. The belt is operated for at least one week in the normal operating state without deviation to calculate the belt width and central co-ordinates in various images, and the means are used as the reference bandwidth W_b and runway central co-ordinate O. In engineering practice, these two basic parameters need to be calibrated at intervals, and the site management engineers are responsible for determining the interval length based on practical experience.

The overall offset E_s of the conveyor belt is expressed by the ratio of the distance between circumscribed rectangle central co-ordinate O_1 and runway central co-ordinate O to the belt width W_b. Exploiting the geometric relationship in fig. 3, the computational formula for global offset is derived:

$$E_s = \frac{|Lx + Rx - 2O|}{2W_b} 100\% \tag{5}$$

In fig. 3(a), Lx = 91 px, Rx = 402 px, W_b = 311 px and O = 256 px. The global offset E_s is calculated to be 3.06%.

Deviation degree quantification and deviation fault identification

During operation, the conveyor belt often undergoes instantaneous deflection, which returns to normal after a period of time. This is a normal phenomenon. To avoid problems like false alarms upon instantaneous drastic deflection of the conveyor belt, severe deviation with-

out reaching alarm threshold and prolonged deviation without alarming, the deviation degree is used as a measure herein to identify the deviation faults of global offset. Assuming two identification thresholds of deviation fault are L_1 and $L_1(L_1 < L_2)$, when the global offset is less than or equal to L_1, it belongs to the normal defection within the allowable range, with a deviation degree of 0. When the global offset is continuously greater than L_1, the accumulated deviation at the i^{th} moment $A(i)$ is calculated by:

$$A(i) = \begin{cases} E_s(i)L_f + A(i-1), \text{ when } L_1 < E_s(i-1) < L_2 \\ E_s(i)L_f, \text{ others} \end{cases} \tag{6}$$

where $E_s(i)$ is the global offset corresponding to the i^{th} moment, $A(i-1)$ – the accumulated deviation corresponding to the i–1^{st} moment, and L_f is the distance travelled by conveyor belt within the time range Δt of image acquisition per frame. Its expression is:

$$L_f = \Delta t V = \frac{HV}{f_{\text{line}}} \tag{7}$$

where H is the image height per frame, V – the travel speed of conveyor belt, and f_{line} – the line frequency of line camera. The accumulated deviation $A(i)$ can be understood as the continuous deviation length corresponding to the case of continuous belt deviation. Longer continuation of deviation indicates faster travel of the conveyor belt and larger length of continuous deviation.

When the global offset at a certain moment is greater than L_1 but discontinuous, the accumulated offset returns to 0. When the global offset at a certain moment is greater than L_2, the deviation degree takes the maximum value A_0. To sum up, the deviation degree $DL_s(i)$ of the conveyor belt at a certain time moment is:

$$DL_s(i) = \begin{cases} 0, & \text{when } E_s(i) \le L_1 \\ A(i) & \text{when } L_1 < E_s(i) < L_2 \\ A_0 & \text{when } E_s(i) \ge L_2 \end{cases} \tag{8}$$

After repeated experimentations, in accordance with the GB/T10595-2009 Standards for Belt Conveyors, the primary offset threshold L_1 is set to 5%, the secondary offset threshold L_2 is set to 15%, and A_0 to 10. These thresholds can be appropriately adjusted as per actual conditions.

Experimental tests are conducted repeatedly with laboratory conveyor, where the deviation degree thresholds T_{h1} and T_{h2} are set to 40 mm and 70 mm, respectively. When the deviation degree is greater than 40 mm and less than 70 mm, an alarm is given, and when the deviation degree is greater than 70 mm, an alarm is given and the conveyor is halted. In actual field applications, the primary and secondary offsets of deviation, and the alarming and shutdown thresholds of deviation degree can be adjusted as per actual in-situ conditions.

Analyses of results

To examine the real-timeliness and accuracy of deviation fault detection, image capturing is performed on the conveyor belt with a global offset of 5% that is running at 0.72 m/s, 1.08 m/s, 1.44 m/s, 1.80 m/s, and 2.16 m/s, respectively. Figure 4 details the deviation states of the conveyor belt. The image resolution is 2048 × 1024 during capturing, and for each im-

Figure 4. Deviation fault test

age, 5 rows of data are extracted at equal intervals for computation of global offset. Analysis is performed herein on the image data with an acquisition duration of 30 seconds.

Experimental analysis at an identical camera line frequency

At different rotation speeds, the line frequency of line camera is set to 1600 Hz for capturing the conveyor belt images and calculating their global offsets. Table 1 lists the results of global offset analysis. According to the table, the mean global offsets are very close to the true values at different speeds, showing relative errors within 5%. The computational duration of image data sampled for 30 seconds is less than 750 ms, and the mean time consumed per frame image is 14.9 ms. Obviously, both the accuracy and real-timeliness of global offset analysis for conveyor belt deviation can meet the operating requirements.

Table 1. Global offset analysis at the same line frequency and different speeds

Speed [ms^{-1}]	Mean global offset [%]	Relative error [%]	Total time consumption [ms]	Mean time consumption per frame [ms]
0.72	4.8267	3.5904	697.3	14.8
1.08	4.9145	1.7397	729.0	15.5
1.44	4.8200	3.7344	701.2	14.9
1.80	4.8516	3.0588	692.7	14.7
2.16	4.7828	4.5413	698.7	14.8

The deviation degrees of the conveyor belt are calculated, and relevant results are plotted as shown in fig. 5. At various speeds, the deviation degrees all range between 40-50 mm. Clearly, the deviation degree measurements are almost unaffected by the change of rotation speed. The system gives an alarm when all the deviation degree values are above 40 mm and below 70 mm.

Experimental analysis at different camera line frequencies

In this experiment, the line camera captures the conveyor belt images at different line frequencies, which are used to calculate the global offsets of the conveyor belt. Table 2 lists the relevant analytical results. As can be seen, the mean global offsets are very close to the true values at different line frequencies and rotation speeds, showing relative errors within 5%. The computational duration of image data sampled for 30 seconds is less than 1.5 seconds, and the mean time consumed per frame image is 16.3 ms.

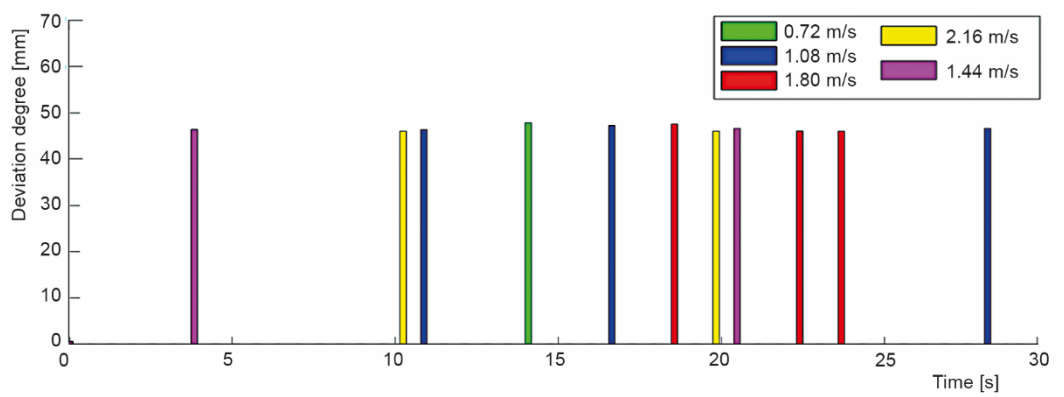

Figure 5. Deviation degree curves at the same line frequency and different speeds

Table 2. Global offset analysis at different line frequencies and speeds

Speed [ms^{-1}]	Line frequency [Hz]	Mean global offset [%]	Relative error [%]	Total time consumption [ms]	Mean time consumption per frame [ms]
0.72	800	4.8072	4.0107	377.4	15.7
1.08	1200	4.8649	2.7770	579.7	16.6
1.44	1600	4.8274	3.5754	769.4	16.4
1.80	2000	5.0184	0.3667	917.2	15.5
2.16	2400	4.9577	0.8532	1242.6	17.5

The deviation degrees of the conveyor belt are calculated, and the relevant results are plotted as shown in fig. 6. At various line frequencies and speeds, the deviation degrees all range between 40-50 mm. Clearly, the deviation degree measurements are unaffected by the change of rotation speed and line frequency, revealing good computational stability. The system gives an alarm when all the deviation degree values are above 40 mm and below 70 mm.

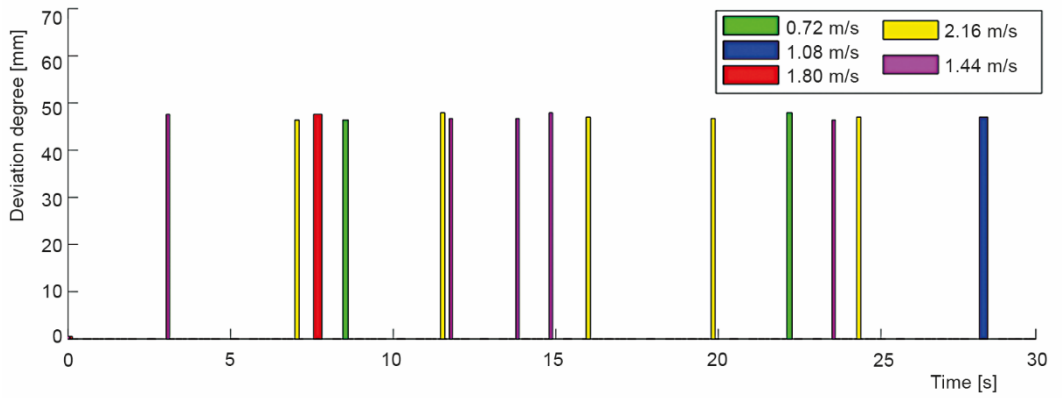

Figure 6. Deviation degree calculations at different line frequencies and speeds

According to a combination of tabs. 1 and 2, the mean time consumption per frame during deviation fault detection is 16.3 ms, and the relative error of global offset computation is within 5%. This indicates that both the accuracy and real-timeliness of deviation fault identification for the conveyor belt can meet the engineering requirements.

Conclusion

In this study, a segmentation model for the conveyor belt images is developed by exploiting the feature of identical illumination received by the same acquisition unit of linear CCD camera at different times. It allows adaptive segmentation of the conveyor belt images by resolving the adaptive segmentation parameters based on the artificial bee colony algorithm, thereby allowing accurate extraction of the belt edge position information. A belt offset quantification model is proposed, which allows accurate calculation, with relative errors below 5%. The proposed model provides an objective basis for the accurate identification of belt deviation faults, as well as an effective approach to the continuous fault monitoring. The technology has opened the path for a new way to continuous on-line detection of the conveyor belt deviation.

Acknowledgement

This work was financially supported by scientific research start-up fund of the Inner Mongolia University of Technology, and technically supported by Inner Mongolia Daban Power Generation Co., Ltd. The authors express gratitude to anonymous reviewers for their comments on the manuscript.

References

[1] Li, W. H., *et al.*, Research on Image Recognition Technology of Belt Conveyor in Coal Mine (in Chinese), *Coal Technology, 39* (2020), 1, pp. 177-179
[2] Mei, X. Z., *et al.*, On-Line Intelligent Evaluation of the Fatigue State of a Composite Conveyor Belt, *Thermal Science, 25* (2021), 3B, pp. 2189-2196
[3] Yin, Z. M., *et al.*, Study on Deviation of Conveyor Belt Based on Multi-Body Dynamics Characteristics (in Chinese), *Journal of Mechanical Engineering, 56* (2020), 1, pp. 37-46
[4] Fu, T., Design of Belt Conveyor Rectification System Based on Machine Vision (in Chinese), *Coal Mine Machinery, 41* (2020), 8, pp. 183-185
[5] Wang, P., Real-Time Monitoring Technology of Conveyor Belt Deviation State Based on Digital Image Processing (in Chinese), *Coal Mine Machinery, 42* (2021), 02, pp. 168-170
[6] Gao, R., *et al.*, Adaptive Multi-View Image Mosaic Method for Conveyor Belt Surface Fault On-line Detection, *Applied Sciences, 11* (2021), 6, pp. 2564-2589
[7] Zhang, M., *et al.*, A Computer Vision Based Conveyor Deviation Detection System, *Applied Sciences, 10* (2020), 7, pp. 2402-2411
[8] Zeng, C., *et al.*, Real-Time Conveyor Belt Deviation Detection Algorithm Based on Multi-Scale Feature Fusion Network, *Algorithms, 12* (2019), 10, pp. 205-216
[9] Yang, Y., *et al.*, On-Line Conveyor Belts Inspection Based on Machine Vision, *Optik, 125* (2014), 19, pp. 5803-5807
[10] Yang, L. S., *et al.*, On-Line Detection of Conveyor Belt Deviation Fault Based on Image Processing (in Chinese), *Coal Engineering, 52* (2020), 10, pp. 116-120
[11] Han, T., *et al.*, Detection Method of Coal Quantity and Deviation of Belt Conveyor Based on Image Recognition (in Chinese), *Industry and Mine Automation, 46* (2020), 4, pp. 20-25
[12] Wang, S. Q., *et al.*, Prediction of Myelopathic Level in Cervical Spondylotic Myelopathy Using Diffusion Tensor Imaging, *Journal of Magnetic Resonance Imaging, 41* (2015), 6, pp. 1682-1688
[13] Yu, W., *et al.*, Morphological Feature Visualization of Alzheimer's Disease via Multidirectional Perception GAN, *IEEE Transactions on Neural Networks and Learning Systems*, On-line first, https://doi.org/10.1109/TNNLS.2021.3118369, 2021

[14] You, S. R., *et al.*, Fine Perceptive Gans for Brain MR Image Super-Resolution In Wavelet Domain, *IEEE Transactions on Neural Networks and Learning Systems*, On-line first, https://doi.org/10.1109/TNNLS.2022.3153088, 2022
[15] Wang, S. Q., *et al.*, Skeletal Maturity Recognition Using a Fully Automated System with Convolutional Neural Networks, *IEEE Access*, *6* (2018), June, pp. 29979-29993
[16] Wang, S. Q., *et al.*, An Ensemble-Based Densely-Connected Deep Learning System for Assessment of Skeletal Maturity, *IEEE Transactions on Systems, Man, and Cybernetics: Systems, 52* (2020), 1, pp. 426-437
[17] Hu, S. Y., *et al.*, Cross-Modality Synthesis from MRI to PET Using Adversarial U-Net with Different Normalization, *Proceedings*, International Conference on Medical Imaging Physics and Engineering, Shenzhen, China, 2019
[18] Wu, K., *et al.*, 3D convolutional Neural Network for Regional Precipitation Nowcasting, *Journal of Image and Signal Processing, 7* (2018), 4, pp. 200-212

Paper submitted: December 25, 2021
Paper revised: June 5, 2022
Paper accepted: June 15, 2022